Zoological Studies **64:**46 (2025)

Updated Redescription and Transcriptomic Insights into *Anthopleura nigrescens* (Verrill, 1928) (Cnidaria, Actiniaria) from Shallow-water Hydrothermal Vents at Kueishan Island and Rocky Shores in the Western Pacific

Meifang Lin[1,*] and YAP Wei Liang Nicholas[2,3]

[1]*Department of Marine Biotechnology and Resources, National Sun Yat-sen University, No. 70, Lien-hai Road, Kaohsiung, Taiwan 804201. *Correspondence: E-mail: meifang.lin@mail.nsysu.edu.tw (Lin)*

[2]*Tropical Marine Science Institute, National University of Singapore, S2S Building, 18 Kent Ridge Road, Singapore 119227. Correspondence: E-mail: yapwln@nus.edu.sg (Yap); cosmogony84@gmail.com (Yap)*

[3]*St. John's Island National Marine Laboratory, c/o Tropical Marine Science Institute, National University of Singapore, 18 Kent Ridge Road, Singapore 119227*

(Received 6 March 2024 / Accepted 16 July 2025 / Published -- 2025)
Communicated by Chien-Hsiang Lin

ORCiD:
Meifang Lin : https://orcid.org/0000-0001-5568-9595
YAP Wei Liang Nicholas: https://orcid.org/0000-0003-4796-1696

Anthopleura nigrescens (Verrill 1928) is a common sea anemone typically encountered in the rocky crevices of shallow-water intertidal zones in the West Pacific. Despite its ubiquity, little is known about the biology of this species, with research on them hindered due to difficulties in distinguishing Indo-Pacific *Anthopleura* species. The original description of *A. nigrescens* was sparse, and while there have been two focused redescriptions of this species, data presented in those accounts were conflicting (*e.g.*, acrorhagi appearance and cnidom), thus the species cannot be identified accurately. In this study, we report the unusual occurrence of *A. nigrescens* beside hydrothermal vents in Taiwan and conducted transcriptomic analyses to better understand the adaptive biology of this species. We also performed a contemporary redescription of *A. nigrescens*, integrating morphological and molecular evidence from both museum specimens and fresh material collected from Taiwan and Singapore, while also incorporating data from earlier descriptions of the species. Transcriptomic analyses revealed a unique *A. nigrescens* adaptive strategy, characterized by the enrichment of metal ion binding genes and the activation of thermal resistance pathways, enabling adaptation to the hydrothermal vent environment compared to individuals inhabiting intertidal shores. Transcriptomic data also provided additional insights to the systematics of *Anthopleura* Duchassaing & Michelotti, 1860, concurring to previous observations that biogeographic patterns are a good predictor of its phylogeny than the current state of the genus'

taxonomy. Overall, while we found that taxonomic characters of material we had examined to agreed, we also found intra-specific morphological deviations particularly concerning occurrence of cnidae documented for the species. Collectively, our findings refined our understanding of the species' taxonomy and support its placement within a biogeographically coherent clade, contributing to a broader understanding of its evolutionary and ecological context.

Keywords: Actinioidea, Anthozoa, Indo-Pacific, Hydrothermal vent, Shallow intertidal, Transcriptome

Citaion: M Lin, Nicholas YWL. 2025. Updated redescription and transcriptomic insights into *Anthopleura nigrescens* (Verrill, 1928) (Cnidaria, Actiniaria) from shallow-water hydrothermal vents at Kueishan Island and rocky shores in the Western Pacific. Zool Stud **64:**46.

BACKGROUND

Sea anemones are a remarkable group of marine invertebrates, with a lineage of approximately 470 million years old (Han et al. 2010; Rodríguez et al. 2014). Like their scleractinian relatives, sea anemones are involved in ecologically important processes, such as being hosts to symbiotic micro/ macrofauna such as dinoflagellates, crustaceans, and fishes (Dunn 1981; Bruce 2005; Sungawa et al. 2009). Part of the success of these marine invertebrates is their ability to thrive in a diverse range of habitats worldwide: ranging from tropical shallow-waters, polar seas, deep-sea trenches, and as mentioned earlier, hydrothermal vents (Fautin 1984; Riemann-Zürneck 1986; England 1987; Goffrendi et al 2021).

While the genus *Anthopleura* Duchassaing de Fonbressin & Michelotti 1860, may be one of the most cosmopolitan sea anemone taxon, with over 40 nominal species reported across the globe (Fautin, 2016; WoRMs). Members of this genus typically inhabit intertidal shores in both temperate and tropical regions (*e.g.*, *Anthopleura elgantissima* (Brandt, 1835) and *Anthopleura buddemeieri* Fautin, 2005, respectively) and are seldom found near hydrothermal vents. However, the presence of *Anthopleura* species near a shallow-water vent in Taiwan was first documented by Chan et al. (2016), who observed a gradual decrease in sea anemone abundance from the vent core to adjacent waters. Subsequently, Chang et al. (2018) also reported their occurrence in this habitat. More recently, Wang et al. (2022) demonstrated that carbon and nitrogen stable isotope signatures differed between central and peripheral vent populations, suggesting a shift in dietary sources between these regions. These findings collectively support a unique ecological resilience of *Anthopleura* to the

vent environment. Given that eight other sea anemone genera have been historically reported to be associated with hydrothermal vents (*i.e.*, *Actinostola* Verrill, 1883; *Alvinactis* Rodríguez, Castorani and Daly, 2008; *Liponema* Hertwig, 1882; *Maractis* Fautin and Barber, 1999; *Ostiactis* Rodríguez, Barbeitos, Daly, Gusmão and Häussermann, 2012; *Pacmanactis* López-González, Rodríguez and Segonzac, 2005; *Paranthosactis* López-González, Rodríguez, Gili and Segonzac, 2003; *Relicanthus* Rodríguez and Daly, 2014), the occurrence of *Anthopleura* sea anemones near these geologic structures are unusual. During scuba surveys near a coastal, shallow-water hydrothermal vent off Kueishan Island in Taiwan, like Chang et al. (2018) and Wang et al. (2022), we too encountered several individuals of *Anthopleura* occurring close to the vent. On our intertidal surveys of a shore nearby, we encountered more individuals of this same species. We identify the species as *Anthopleura nigrescens* (Verrill 1928). Given the unique occurrence of this species across two vastly different habitats, this distribution raises questions about potential physiological plasticity that may enable individuals to thrive under varying environmental conditions, warranting further investigation.

Hydrothermal vents are common geologic structures, commonly found in tectonically active regions such as mid-ocean ridges, back-arc basins, and volcanic areas. These vents are areas where geothermally heated, mineral-rich seawater is released through cracks and fissures in the seabed (Holden et al. 2014; Colín-García et al. 2016). Hydrothermal vents can be found in both shallow and deep waters (*e.g.*, Tarasov et al. 2005; Escobar-Chicho et al. 2019; Liu et al. 2024); the former occurring nearer to coastlines while the latter are typically found further away, exceeding depths of around 2000 m. Significantly more research has been conducted on deep-water hydrothermal vents than on those in shallow waters, largely because deep-sea vents were discovered earlier (Wang et al. 2022). The ecology of shallow-water hydrothermal vents remains understudied, although efforts to better understand these ecosystems have increased in recent years (*e.g.*, Eythorsdottir et al. 2016; Chang et al. 2018; Wang et al. 2022). Despite the differences in research attention between shallow-water and deep-sea hydrothermal vents, these geologic structures are recognized as dynamic and ecologically important marine ecosystems. Some geobiologists – though the hypothesis remains controversial due to limited evidence – have proposed that such vents may have served as sites for the origin of life (*e.g.*, Wächtershäuser 1988; Holm and Andersson 2005). Hydrothermal vents support diverse communities of marine invertebrate fauna, among them are sea anemones (Cnidaria, Actinaria) (Fautin, 1984; Chang et al. 2018; Wang et al. 2022).

In attempting to confirm the identity of the sea anemone encountered for further research on its adaptive biology, we found that previous detailed taxonomic accounts of *A. nigrescens* were conflicting, hindering confident identification, particularly with respect to the species' acrorhagi and cnidom (= inventory of cnidae, see Fautin 2009: 1054). Although comprehensive species

descriptions were provided by Dunn (1974) and England (1987), based on materials from Australia, Hawaii, Hong Kong, and India, their accounts present conflicting diagnostic features. For example, Dunn (1974: 377) (and later as DG Fautin in Fautin et al. 2009, although the description in this checklist was brief, using materials only from Singapore, and repeatedly references Dunn 1974) indicated that the presence of "… White-tipped acrorhagi…" as a diagnostic character. However, this feature is not mentioned by England (1987) in his material. Beyond this, England (1987) also reported differences in the number of tentacles, sphincter size, and cnidom type and size compared to Dunn's description. Notably, England (1987) did not include illustrations of the external morphology, making it difficult to assess whether his specimens were indeed *A. nigrescens* exhibiting morphological variations. Moreover, some of England's identifications have been questioned in later studies (see Yap et al. 2021). To reconcile these discrepancies, we incorporated both morphological re-examination and molecular analyses of our specimens, allowing us to confidently assign them to *A. nigrescens* based on genetic and diagnostic features.

Thus, our study aims to better understand the adaptive biology of *A. nigrescens* by comparing individuals from intertidal shores with those from shallow-water hydrothermal vents. Specifically, we investigate whether differences in gene expression profiles reflect habitat-specific adaptations and whether these differences suggest potential physiological plasticity. In doing so, we provided detailed transcriptomic data, uncovering biological processes and gene expression patterns associated with the contrasting habitats from which the individuals were collected. Additionally, we revisited the species boundaries proposed by Dunn (1974) and England (1987) to determine whether *A. nigrescens* represents a single, widely distributed species, by integrating new field and morphological observations from Taiwan, Saudi Arabia, and Singapore, along with molecular data from Taiwan and Singapore. *Anthopleura* species have also served as model organisms for studying toxins, thermal stress, and symbiosis between sea anemones and microorganisms, as reviewed by Daly et al. (2017) and Macrander et al. (2018). Our present study builds upon this foundation by contributing new insights into the evolutionary history and ecological significance of members of this genus.

MATERIALS AND METHODS

Specimens examined

Fresh material examined in this study were collected by hand, in some instances using a small mallet and chisel to ease the animals from the surface it was attached. Broadly, animals were

collected from two distinct marine habitats: i) tropical shallow-water intertidal rocky shores (depth < 2 m), and ii) the edges of hydrothermal vents (depth = 15 m). Individuals from the rocky shore were gathered from Saudi Arabia (N = 3), Singapore (N = 3), and Taiwan (N = 6) (referred to as MG), whereas those from the hydrothermal vents (N = 4) (referred to as KI) were only obtained from Taiwan (Fig. S1). Specimens were collected during low tide windows and non-venting phases of tidal cycles to ensure accessibility and minimize environmental variability. Sea anemones were first observed *in-situ*, then photographed.

In the laboratory, collected individuals were relaxed in 7.5% magnesium chloride overnight, before fixation in 10% formalin. Tissue was excised from the tentacles or pedal disc of some individuals prior to fixation. The samples were preserved in absolute ethanol (molecular grade CAS: 64-17-5) for molecular analyses. To infer transcriptomic changes in individuals that live alongside the hydrothermal vents, an additional eight sea anemones were collected from these habitats, then snap-frozen on site in liquid nitrogen for RNA extraction. We note that individuals were selected at similar body sizes to minimize age-related transcriptional variation. While reproductive states were not histologically confirmed, care was taken to avoid visibly spawning individuals. These measures aim to reduce confounding effects and enhance comparability across vent and intertidal populations.

Morphological analyses

Formalin-fixed specimens were first examined whole, then dissected such that both external and internal morphologies of the animal may be studied. To visualize the musculature and mesenterial arrangement of these sea anemones, histological sections, each 8 μm thick, were prepared and stained with Ehrlich's Haematoxylin and Eosin Y (Humason 1967). We characterized the cnidom using squash preparations of tissues obtained from the sea anemone's tentacle tip, acrorhagi, mid-column, actinopharynx and mesenterial filaments. Length and width of undischarged capsules were measured at 1000X. Nomenclature of cnidae follows that of Mariscal (1974).

To affirm that the animals we had collected were indeed *A. nigrescens*, we compared our findings to previous redescriptions of the species (Dunn 1974; England 1987; Fautin et al. 2009), to voucher specimens for which data from these specimens were gathered (*e.g.*, those published in Fautin et al. (2009) that are now housed at the Zoological Reference Collection (ZRC), of the Lee Kong Chian Natural History Museum, National University of Singapore, Singapore), and to the holotype (*i.e.*, *Tealiopsis nigrescens* Verrill, 1928; ANMH 1485; see Fautin 2016), kept at the American Natural History Museum (AMNH), New York City, USA.

All new specimens collected for this study were deposited at the Lee Kong Chian Natural History Museum, National University of Singapore, as part of the Zoological Reference Collection (ZRC).

Phylogeny analyses

Genomic DNA was extracted individually from whole polyps of sea anemones collected from the vent area and the intertidal zone for subsequent phylogenetic analysis. We tested phylogenetic hypotheses presented in Daly et al. (2017), and included additional taxa to the tree (see Table S1). Polymerase chain reaction (PCR) was then conducted for each DNA sample, targeting specific markers including mitochondrial markers (COIII, 12S, and 16S) and one nuclear marker (28S), as outlined in prior studies (Chen et al. 2002; Daly et al. 2008; Geller and Walton 2001). Polymerase chain reaction cycling conditions adhered to the protocols detailed in the cited references. These amplification processes were designed to identify sequences commonly utilized in *Anthopleura* sea anemone phylogenetics.

Sequences were concatenated after alignment using MAFFT (Katoh et al. 2019) for 28S and MUSCLE (Edgar 2004) for mitochondrial genes followed by trimming manually. The alignment on which analyses were conducted consisted of 2,651 base pairs, and the best-fit model applied was GTR+G+I estimated by jModelTest (Darriba et al. 2020). Both maximum likelihood analysis (ML) and Bayesian inference (BI) were carried out; ML phylogenetic analyses were conducted using RAxML (Stamatakis 2014) for 1,000 bootstraps. The final optimization likelihood was -13862.55. BI was performed in MrBayes (Ronquist and Huelsenbeck 2003) for four chains, 10 million generations, checking for convergence as the average split frequency and discarding the first 25% of trees as burn-in. The standard deviation of split frequency after 10 million generations was 0.01. Sequence alignment used in the phylogenetic analyses is provided as supplementary materials.

Transcriptome assembly

Total RNA was individually extracted from eight whole polyps collected at the vent sites using TRI Reagent (Thermo Fisher Scientific), following the manufacturer's instructions. Complementary DNA (cDNA) libraries were prepared for each specimen using the Illumina TruSeq Stranded mRNA Sample Preparation Kit, which includes poly(A) enrichment and barcoding. Libraries were sequenced on the Illumina NovaSeq 6000 platform using 150 base pairs (bp) paired-end reads with S1 flow cell chemistry. A total of 81,915,559 raw reads were generated after sequencing. Quality trimming was conducted using Trimmomatic v.0.39 (Bolger et al. 2014) and

retained reads larger than 80 bp with a quality threshold higher than 30. A total of 57,102,236 clean reads were then used for *de novo* transcriptome assembly using Trinity (Grabherr et al. 2011; Haas et al. 2013), followed by removing transcripts shorter than 300 bp. CD-HIT v.4.8.1 was then implemented to cluster the sequences with 90% similarity (Fu et al. 2012; Li and Godzik 2006). The GC content of the transcriptome was also estimated to check for the existence of the symbiont. To assess the completeness of the transcriptome, Benchmarking Universal Single-Copy Orthologs (BUSCO) searching based on the metazoan v.10 was applied for *A*. *nigrescens* in this study and its counterparts *A. elegantissima* (Macrander et al. 2015) and *A. buddemeieri* (van der Burg et al. 2016). The transcriptome data are available on the NCBI under accession number PRJNA1042849.

Comparative transcriptome analysis

To explore the genetic repertoires of *A. nigrescens*, we further conducted an orthologous search among *A*. *nigrescens, A. elegantissima*, and *A. buddemeieri* using OrthoFinder (Emms and Kelly 2019). The genes were identified into three groups, the Anthgroup contained the orthologous groups (OGs) present in all *Anthopleura* species, the J_group contained OGs present only in *A*. *nigrescens* and *A. buddemeieri,* but absent in *A. elegantissima*, and a group (An_group) contained OGs present only in *A. nigrescens* from this study. The gene ontology (GO) for each group was performed using Blast2GO (Conesa et al. 2005) against the UniProtKB/Swiss-Prot database (accessed on August 20, 2021), with an E-value cutoff of 1e-5; all other annotation parameters were set to their default values within Blast2GO. The enrichment of GO was analyzed using R package topGO (Alexa and Rahnenfuhrer 2024) to determine the significantly enriched GO terms in each dataset with a p-value < 0.05 (Fisher's exact test).

RESULTS

Phylogeny reconstruction

The concatenated dataset used for phylogenetic reconstruction included 92 taxa and consisted of 2,697 aligned sites. The resulting ML tree topology closely resembled those reported by Daly et al. 2017 and Yap et al. 2023, reaffirming the paraphyletic nature of the genus *Anthopleura* (Fig. 1). While several new taxa were incorporated into the analysis (Table S1), nine major clades were identified, broadly corresponding to the clade structure described in Daly et al. 2017. To facilitate comparison and interpretation, we adopt the clade definitions established by

Daly et al. (2017: fig. 2): the A Clade includes South African species and the type species of *Anthopleura*, *Anthopeura krebsi* Duchassaing & Michelotti, 1860; the B clade consists of members of *Bunodosoma* Verrill, 1899, with the exception of the Old World species *Bunodosoma.capsense* (Lesson, 1830); the EA clade includes Northern Hemisphere species of *Epiactis* Verrill, 1869; the EP clade contains three geologically proximate species; the ST clade includes members of Stichodactylidae Andres, 1883 and *Anthopleura thallia* (Gosse, 1854); and the J Clade comprises *Anthopleura* species from the Pacific.

Fig. 1. Phylogenetic tree based on the combined dataset (cox3, 12S, 16S, 28S). Specimens of *A. nigrescens* analyzed in this study are highlighted in bold, and three subgroups within the J clade are indicated in orange. Clade designations follow Daly et al. (2017): the J clade includes species from the Pacific; the A clade comprises South African species; the B clade includes members of *Bunodosoma*; the EA clade contains Northern hemisphere members of *Epiactis* and *Aulactinia*; the EP clade groups three geologically close species; and the ST clade consists of members of Stichodactylidae and *A. thallia*. For a detailed description of each grouping, refer to the Results section. Bootstrap support values from ML and posterior probabilities from BI are shown at

the nodes, in that order. Only bootstrap values > 50, and posterior probabilities > 0.5 are displayed; values below these thresholds are denoted by (-).

The phylogenetic analysis revealed that the *Anthopleura* specimens in this study fall within the "Pacific clade" (= J clade), which encompasses most species inhabiting the Pacific Ocean. This J clade is subdivided into three subgroups: Clade One comprises species from the Northwest Pacific (*Anthopleura atodai* Yanagi & Daly, 2004*, Anthopleura japonica* Verrill, 1899*, Anthopleura kurogane* Uchida & Muramatsu, 1958, and *A.* sp. "*inornate*"), Clade Two consists of species of the genera *Phymanthus* Milne Edwards & Haime, 1851 and *Heteractis* Milne Edwards & Haime, 1851, and Clade Three includes Central to Southwest Pacific species (*Anthopleura handi* Dunn, 1978*, Anthopleura buddemeieri* Fautin, 2005*,* and *A. nigrescens*). Two *A. nigrescens* specimens, one from a venting habitat (KI) and one from a non-venting habitat (MG), were placed within the third clade of the J clade (Fig. 1). Interestingly, these specimens did not group with other *A. nigrescens* counterparts from Hawaii and Galapagos but instead formed a close relationship with those from the shallow-intertidal habitats in Singapore.

Anthopleura. nigrescens Galapagos exhibited a close relationship (81/0.96 for ML resampling bootstrap value and BI posterior probability value, respectively) with those from the A clade – this clade consisted of species from South Africa (*Anthopleura* sp. and *Bunodosoma* sp.), *Anthopleura. pallida* Duchassaing & Michelotti, 1864, *Anthopleura krebsi* Duchassaing & Michelotti, 1860, *Anthopleura wardi* (Carlgren, 1900), *Anthopleura insignis* Carlgren, 1940, and *Bunodosoma capense* (Lesson, 1830), although some relationships remained unresolved. Meanwhile, *A. nigrescens* Hawaii was grouped with *Haloclava producta* (Stimpson, 1856), which was associated with the ST clade as shown in Daly et al. 2017, or with other species in Actinioidea as indicated in Rodríguez et al. 2014.

Sister to the J clade, members of Heteranthidae, *Isactinia* Carlgren, 1900, and *Anthopleura dixoniana* (Haddon & Shackleton, 1893) formed a poorly resolved clade, which was also observed in Yap et al. (2021). *Heteranthus verruculatus* from Singapore formed a single clade (= Heteranthidae clade) but excluded one specimen from the same population. In this phylogenetic tree, *A. dixoniana* was not grouped with the clade that included *Anthopleura ballii* (Cocks, 1851) and *Anemonia viridis* (Forsskål, 1775), as seen in Daly et al. (2017), but situated between the Heteranthidae Carlgren, 1900 clade and an unnamed clade consisting of *Isactinia citina* (Haddon & Shackleton, 1893) and the other *Heteranthus verruculatus* Klunzinger, 1877 from Singapore.

Taxonomic account

Anthopleura nigrescens (Verrill, 1928)

(Table 1, Figs. 2–5)

Tealiopsis nigrescens – Verrill, 1928: 26 [original description]

Cladactella obscura – Verrill, 1928: 24–25 [original description]

Anthopleura pacifica – Uchida, 1938: 305–309 [original description]

Bunodactis nigrescens – Carlgren, 1949: 65.

Anthopleura nigrescens – Mathew, 1967: 41–43; Dunn, 1974: 377–382; England, 1987: 248–250. Fautin et al. 2009 : 127–128.

Type material examined and nomenclatural considerations: Holotype – *Tealiopsis nigrescens* (AMNH 1485), collected by A.E. Verrill 1925 from "… tide pool or under stone" of Nawiliwili Bay, in Kauai, Hawai'i. Name-bearing material comprises of a single, retracted specimen, that has its tentacles partially exposed (Fig. 2A). Entirely reddish brown, material is almost whole; a small longitudinal slice, extending from the distal to the proximal end of the animal, had been removed and is not present in the lot (Fig. 2B). A horizontal, incomplete cut is also present at the mid-column of the material. Internally, the material is choked with white gametogenic tissue (Fig. 2B).

Material examined: Intertidal rocky shore (*observed alive) (Fig. S1).

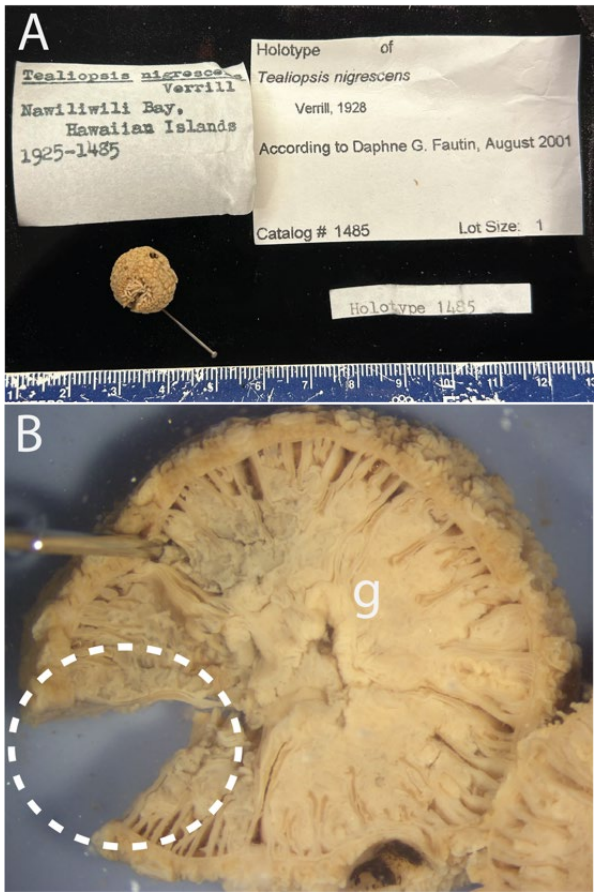

Fig. 2. Holotype of *Tealiopsis nigrescens* Verrill, 1928 (ANMH 1485). A, Whole specimen, top view, with associated labels in the lot. B, Internal appearance of holotype. Note that the gastric cavity is filled with gametogenic tissue, denoted by the letter 'g'. A slice of the anemone removed from the animal. Photo credits: Yap NWL.

Saudi Arabia – Thuwal (ZRC.CNI.1117 X 3*). Malaysia – Perhentian Islands (photographed but not collected). Singapore – Changi Point (ZRC.CNI.0074 X 1); Changi Beach (ZRC.CNI.0232 X 1), (ZRC.CNI.0233 X 1); Pulau Tekukor (ZRC.CNI.1107 X 4*); Punggol Beach (ZRC.CNI.1221 X 6*). Taiwan – intertidal (ZRC.XXXXX. X 6*); hydrothermal vent (ZRC.XXXXX. X 4*).

Redescription: Natural History – Typically in clusters, sometimes solitary (Fig. 3A–C). Animal attaches itself on the surface of rock, or may extend from narrow crevices (Fig. 3A–C). Those near hydrothermal vent range 1 to 35 metres away; those in shallow waters may appear as round, shiny black beadlets during low spring tides (Fig. 3C). Grains of sediment or tiny fragments of shell may cling onto verrucae. Reproduces both sexually and asexually (Fig. 3D; also for the latter, see Dunn 1974). Not associated with dinoflagellates. In the field, we have not seen it associated with any macrofauna. However, AE Verrill (1928) reports it being associated with the crab, *Polydectus cupulifer* (Latreille in Milbert, 1812).

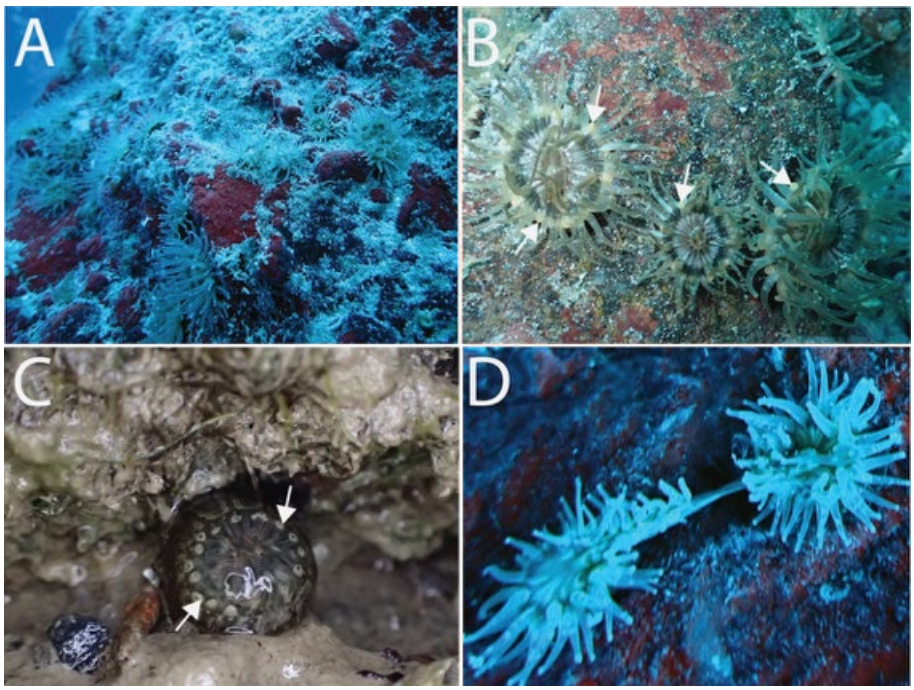

Fig. 3. *In situ* live individuals of *Anthopleura nigrescens*, external morphology. A, A clustered population of *A. nigrescens* occurring near a hydrothermal vent in Taiwan, at a depth of 20 metres. Photo credit: Lin MF. B, Another cluster occurring at a surface of a rock near the venting side, note the white tipped acrorhagi distinct of *A. nigrescens* (arrowed). Photo credit: Lin MF. C, A solitary individual among barnacle tests encountered in a narrow crevice of a storm drain at East Coast, Singapore. White acrorhagi (arrowed) are obvious here too. Photo credit: Yap NWL. D, Two individuals that were the result of a recent, asexual longitudinal split, with the connective tissue still present between these individuals. Photo credit: Lin MF.

Table 1. Cnidom data gathered from published re-descriptions of *Anthopleura nigrescens*: the holotype *Tealiopsis nigrescens* (AMNH1485) that England (1987) had examined, specimens from Hawaii that Dunn (1974) studied, those from elsewhere in the Indo-Pacific that England (1987) had also studied, and from fresh materials gathered for this study. Abbreviations: *N* signifies the proportion of individuals that the cnida type was present out of the total number examined; *n* indicates the number of unfired cnida capsules that were measured; values in parentheses are for single capsules that were outliners to the size range; a short dash "-" denotes that the cnida type was not reported or absent

		Published re-descriptions								This study		
		Holotype *Tealiopsis nigrescens* AMNH 1485* England (1987)		Dunn (1974)			England (1987) and England (1992)			*Anthopleura nigrescens* from Taiwan		
Tissue	Cnidae	Range length x width (um)	*n*	Range length x width (um)	*n*	*N***	Range length x width (um)	*n*†	*N*	Range length x width (um)	*n*	*N*
Tentacles	Spirocysts	14.1–26.4 × 1.8–3.0	-	10.3–28.2 × 1.9–3.8	67	-/10	14.1–31.1 × 1.8–3.3	-	4/4	(8.0)12.0–28.5 × (1.5)2.0–3.5	72	4/4
	Small basitrichs[1]	-	-	-	-	-	12.0–14.4 × 1.2–1.8	-	2/4	-	-	-
	Basitrichs	15.6–20.4 × 1.8–2.4	-	16.0–21.6 × 1.7–2.8	84	-/10	16.6–25.2 × 1.2–2.6	-	4/4	(16.0) 18.0–24.0 × 2.0–3.0	50	4/4
Marginal acrorhagi	Basitrichs	12.0–20.4 × 1.8	-	-	-	-	8.4–20.4 × 1.2–1.8	-	4/4	13.0–17.0 (18.0) × 2.0–3.0	30	2/2
	Holotrichs	-	-	-	-	-	-	-	-	(7.0) 8.0–12.5 × 2.0–3.5	19	2/2
	Atrichs[1,2]	-	-	27.3–43.2 × 2.8–4.7	61	-/10	33.6–58.7 × 3.6–5.4	-	4/4	-	-	-
	Spirocysts	-	-	14.1–28.2 × 1.9–3.6	66	-/10	26.5–36.0 × 2.4 –3.3	-	2/4	-	-	-
Column	Small basitrichs	-	-	11.3–16.0 × 1.7–2.4	59	-/10	9.6–24.0 × 1.8–3.0	-	4/4	12.0–18.0 × 2.0–3.0	30	3/3
	Basitrichs[1,3]/ Heterotrichs[2]	-	-	16.5–22.6 × 2.4–3.8	74	-/10	16.8–24.0 × 3.0–4.0	-	3/4	21.0–25.0 × 3.0–4.0	10	1/3
Actinopharynx	Small basitrichs/ Basitrichs[2]	9.6–12.0 × 1.8	-	-	-	-	9.6–16.2 × 1.8–2.0	-	4/4	13.0–15.0 × 2.0–2.5	10	1/2

	Basitrichs	21.6–26.4 × 2.5–3.0	-	20.7–27.3 × 1.9–2.8	53	-/10	17.2–29.8 × 2.0–3.3	-	4/4	(20.5)23.0–28.0 × 2.0–4.0(4.5)	20	2/2
	Microbasic amastigophores[2]	19.2–24.0 × 3.0–3.6	-	-	-	-	19.0–27.1 × 3.0–5.3	-	4/4	-	-	-
Mesenterial filaments	Small basitrichs	10.8–18.0 × 1.8	-	13.2–18.7 × 1.7–2.6	62	-/10	10.8–15.5 × 1.8–2.4	-	4/4	11.0–16.0 × 2.0–3.0	22	2/2
	Basitrichs	27.6–31.2 × 3.6–4.2	-	20.7–29.1 × 2.4–3.8	36	-/10	22.8–31.2 × 3.3–4.8	-	4/4	14.0–17.0 × 2.0–3.0	10	1/2
	Microbasic *p*-mastigophores	-	-	15.0–18.8 × 2.8–4.7	37	-/10	9.6–17.9 × 2.4–3.0	-	3/4	-	-	-
	Microbasic amastigophores	18.0–21.6 × 3.6	-	-	-	-	15.6–27.1 × 3.0–5.3	-	4/4	-	-	-

[1]Cnida type reported in England (1987). [2]Cnida type reported in Dunn (1974). [3]Cnida type reported in this study. *England (1987) erroneously states that this specimen, AMNH1485, to be a 'paratype'. Fautin (2016: 320) documents this specimen to be the holotype; in studying the same specimen, the labels in its jar (*i.e.,*, Fig. 2), and following Verrill's (1928: 26) declaration that the "… Type specimen in the American Museum of Natural History, Catalog No. 1485," , we concur with Fautin (2016). **While Dunn (1974: 377) [=Fautin DGF] indicates the number of individuals (*i.e.*,, 10) that she had characterized the cnidom from, she did not indicate the proportion of individuals for which these cellular products were found from – this was an early work of hers. Proportion of individuals for which a cnidae type may occur in a sample is seen in her latter publications (*e.g.*, Dunn, 1981; Fautin, 2005). †The number of unfired cnidae capsules that were measured by KW England in both his 1987 and 1992 publication were not explicitly stated by him.

Tentacles: Number range between 36 to 167 (see Dunn 1974; England 1987), typically up to 48 in symmetrical polyps. Arranged one per endo-/ exocoel, in three cycles. Innermost approximately 3/5 in length of oral disc diameter; outmost shortest, 2/3 length of innermost. In life, innermost raised vertically when expanded, those in remaining cycles splayed horizontally, may hang over margin (Fig. 4A, B). Extends and retracts readily; form simple, slim, wide at base and narrows to a point (Fig. 4A, B). Tip blunt and slightly knobbed, perforated. When preserved, may appear elongated (Fig. 4C) or as a stout cone (Fig. 4D). In life, translucent grey in colour with a pinkish/reddish or grey cast, white spots present on oral side (Figs. 3B and 4A, B), may appear entirely white when photographed underwater (Fig. 3A, D); entirely white or reddish-brown in colour in preserved specimens (Fig. 4C, D).

Oral disc: Outline round, flat when animal expands in life (Fig. 3B). Thin-walled, in life, same colour as tentacles (Fig. 3B); in preserved specimens, entirely see-through (Fig. 4D). Dark radial lines present, extending from mouth to margin, corresponding to mesenterial insertions (Fig. 3B). In life, radial lines appear thicker with dark-reddish cast (Fig. 4A); in preserved material, as very thin lines. Central-mouth oval in outline, flat, actinopharynx may be slightly pushed out. When alive, edge of mouth with dark-brown cast (Fig. 3B); no such colouration is seen in preserved materials.

Column: Fosse present, deep. Column wall thin; mesenterial insertions seen as thin-white lines extending from distal to proximal end, dark brown lines may be present corresponding to mesenterial insertions (Fig. 4A, B). Distal end crowned with inflated acrorhagi, resembling fat fingers, endocolic, not perforated (Fig. 4A–D). In expanded individuals, distal end flared outwards and is wider than proximal end (Fig. 4A). Extending from distal to proximal end, longitudinal rows of verrucae are present (Fig. 4C, D). Verrucae round in outline, edges thickened, middle thin-walled; approximately 1mm in diameter, endocoelic (Fig. 4E). Up to 10 verrucae per row; tip of acrorhagi anointed with a single verruca (Fig. 4C, D). In life, acrorhagi typically white-tipped or of lighter colour shade, most obvious when expanded.

Pedal disc: Overall circular in outline; irregular circular round in some individuals (Fig. 4F). Flat with scalloped edge. Thin-walled, easily ruptured resulting in mesenterial filaments spilling out. Mesenterial insertions visible as dark radial lines, arrayed outwards (Fig. 4F); lines thicker in live individuals, thinner in preserved materials. Light brown in live animals; cream-white in preserved specimens.

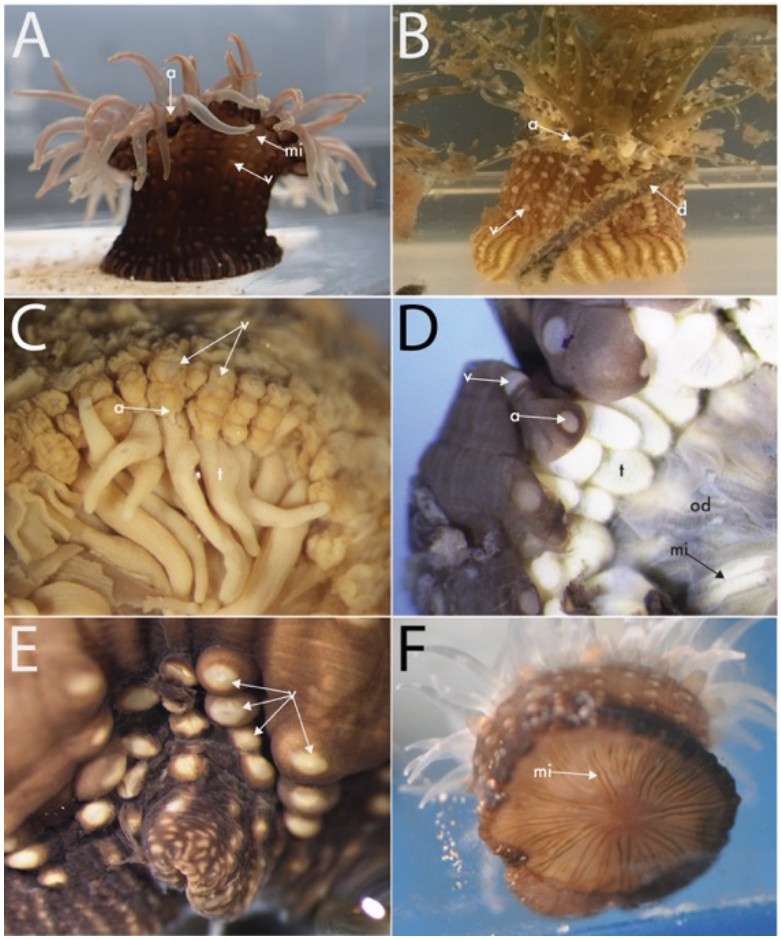

Fig. 4. External morphology of *Anthopleura nigrescens*, live and fixed individuals. A and B, Expanded individuals from Taiwan and Saudi Arabia respectively, side view. Note: i) how innermost tentacles are raised and those of outermost are overhanging; ii) the difference in column colour (perhaps geographical?), however distinct white acrorhagi remains. C, holotypec(AMNH 1485), close-up of column distal-end to show verrucae and acrorhagi, top view. Note the similarity of structures to specimen from Taiwan, presented in D. D, Close up of the acrorhagi and tentacles of a fixed individual, top view. E, Close up of verrucae. F, View of pedal disc. Abbreviations: a, acrorhagi; d, debris; mi, mesenterial insertion; od, oral disc; v, verrucae. Photo credits: Lin MF and Yap NWL.

Internal morphology: Marginal and oral stomata present. Actinopharynx extends up slightly past mid-column, pleated longitudinally, white in life, cream-coloured in fixed materials. Up to 24 pairs of mesenteries in symmetrical individuals, arrayed in three cycles (*i.e.*,, 6 + 6 + 12), although arrangement and numbers vary in clones. Completeness of mesenteries varies; in symmetrical individuals first two cycles typically complete. Gametogenic tissue may be attached to all mesenteries. Number of siphonoglyphs two in symmetrical individuals, may vary in clones. Siphonoglyphs usually not attached to directives, but in one individual (ZRC.XXXX 6*) we found it to be attached. Retractor muscle diffuse, strong, extends the entire ridge of lamellae. Slight lip present at one end of retractor. Parietobasilar muscle well-developed in first two mesentery cycles, with pennon (Fig. 5A). Sphincter muscle present, weakly circumscribed (Fig. 5B). Fosse present, deep.

Cnidom: Spirocysts, basitrichs, b-mastigophores, holotrichs, p-mastigophores. Differences in cnidae sizes and tissue distribution between individuals from the shallow intertidal and hydrothermal vent are shown in table 1.

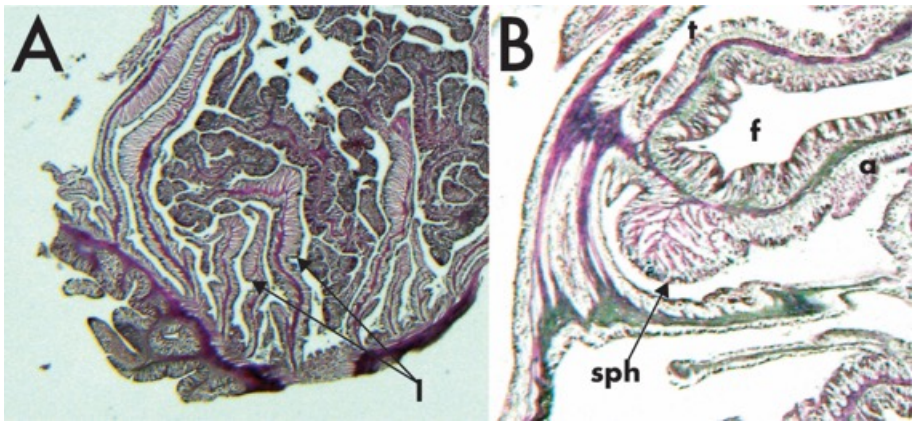

Fig. 5. Internal morphology of *Anthopleura nigrescens* from Taiwan. A, mesenteries of an individual, cross section at mid-column. The retractor muscles are diffused and slightly circumscribed, note the presence of the lip present in stronger muscles. B, sphincter muscle of an individual, transverse section at the distal end. Note its conspicuous and restricted appearance. Abbreviations: a, acrohagi; f, fosse; l, lip; sph, sphincter. Photo credits: NWL Yap.

Transcriptomics

To advance understanding of the genetic characteristics of *A. nigrescens* and enrich the genetic resources available for the genus *Anthopleura*, a *de novo* transcriptome of *A. nigrescens* from the KI population was developed. It contains 61,632 contigs and 33,061 predicted proteins (Table 2). The N50 was 1,582 bp and the BUSCO completeness rate was 89.5%. These assessments indicated that this assembly is comparable to the transcriptomes of other *Anthopleura* species. In comparison to the transcriptomes of the well-studied species *Anthopleura elegantissima* (Brandt, 1835) in the Atlantic Ocean and *A. buddemeieri* in the West Pacific Ocean, the result of the completeness analysis indicated that this assembly contains almost 90% of the expected single-copy genes with a low duplication score, suggesting that this transcriptome is high-quality. This transcriptome is the most comprehensive *Anthopleura* dataset to date, providing a valuable genetic resource from one of the scarce cnidarians documented in vent environments, particularly within the Pacific Ocean (Fig. 6A).

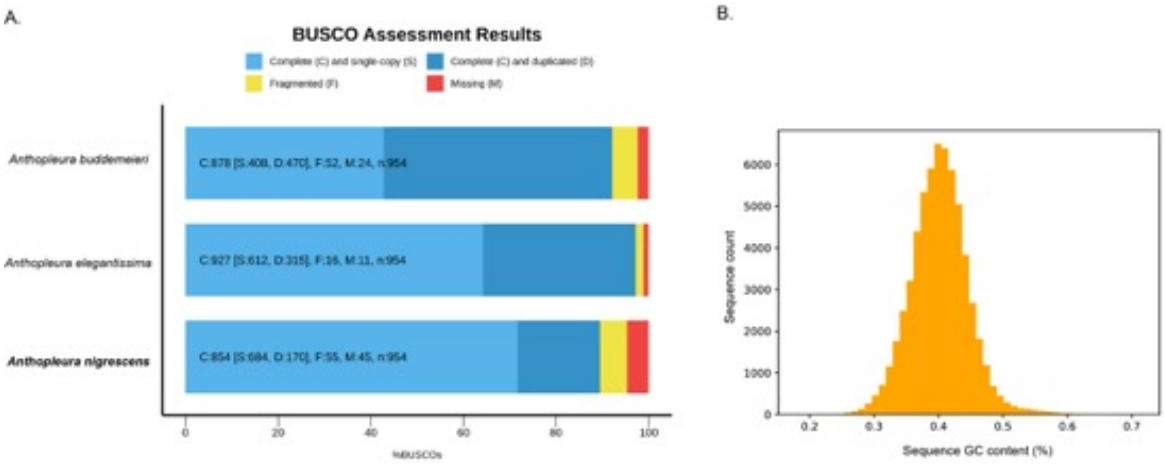

Fig 6. The assessment of *Anthopleura nigrescens* transcriptome. A, The BUSCO assessment of *Anthopleura nigrescens*, *A. buddemeieri*, and *A. elegantissima* transcriptomes. The BUSCO datasets of the metazoan odb10 with 954 BUSCOs were used to assess the transcriptome assemblies. B, The distribution of GC content in the sequences of *A. nigrescens* transcriptome assembly.

Table 2. Statistics of transcriptome assembly of the *Anthopleura* inhabiting vent

Number of raw reads pairs	81,915,559
Number of clean read pairs	57,102,236
Number of assembled bases	66,484,005
Number of contigs	61,632
N50 (bp)	1,582
Mean length (bp)	1,078
GC content	40.6%
Number of proteins	33,061

The homology search results indicated the absence of Symbiodiniaceae sequences within the assembly. Additionally, the analysis of GC content distribution analysis revealed a singular pick at around 41%, aligning with typical ranges observed in cnidarians (*e.g.* Guzman et al. 2018). Given that Symbiodiniaceae tend to exhibit higher GC content, these findings confirm that the *Anthopleura* species under investigation is non-symbiotic. This result suggested that this species does not depend on Symbiodiniaceae endosymbiosis for its nutritional needs (Fig. 6B).

Comparative transcriptomics

Out of a total of 43,532 OGs identified, 15,603 OGs (21,381 transcripts) were commonly present in three *Anthopleura* species, while 4167 OGs (5,332 transcripts) were found in *A. nigrescens* and *A. buddemeieri* belonging to the J clade, and 510 OGs (1,324 transcripts) were exclusively found in *A. nigrescens* (Fig. 7). *Anthopleura nigrescens* exhibited a higher number of

enriched GOs, including metal ion binding (GO:0046872), phosphatidylcholine biosynthetic process (GO:0006656), vesicle transport along actin filament (GO: 0030050), (GO:0005524), myosin complex (GO: 0016459), and dynein intermediate chain binding (GO:0045505), all statistically significantly enriched ($p < 0.05$, Fisher's exact test). These enriched GO terms likely reflect the organism's adaptation to the vent environment for thermal resistance and influence from the metal in the vent fluid (see discussion). In the J clade species, membrane-bounded organelle (GO:0043227), peptidoglycan catabolic process (GO:0043227), and lysozyme activity (GO:0003796) are relatively enriched, indicating an important role in anti-pathogen defense and highlighting the significant influence of microbial association in these species. Additionally, GO terms related to general biological processes, such as primary metabolic process (GO:0044238), mitochondrion (GO:0005739), nucleus (GO:0005634), catalytic activity (GO:0003824), and DNA binding (GO:0003677), were consistently enriched to a similar extent in all sea anemones, suggesting their involvement in the general functions of *Anthopleura* sea anemones.

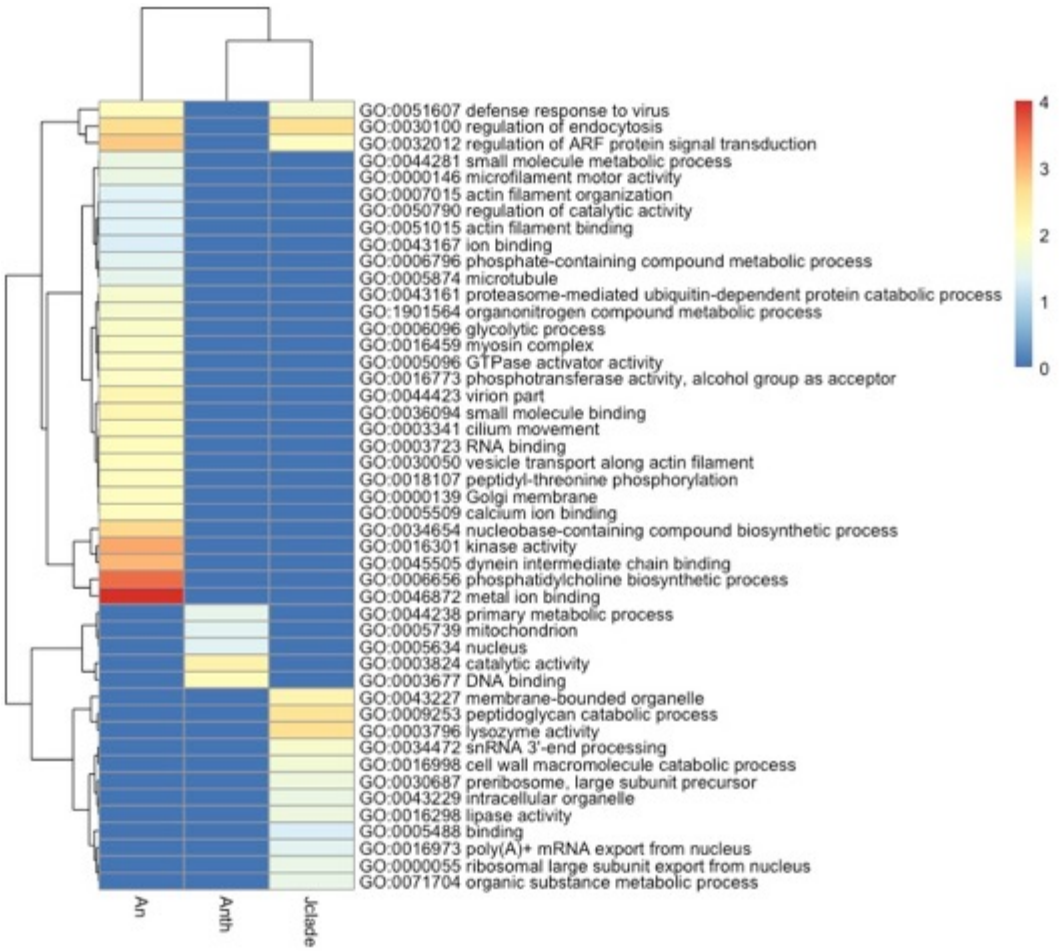

Fig. 7. Enriched gene ontology (GO) analysis for *Anthopleura* species transcripts classified by origin. Only selected GO terms with enrichment *p*-values (*p*-value < 0.05, Fisher's exact test) are shown. An: *A. nigrescens*-specific gene sets ($n = 4$); Anth: gene sets present in *A. nigrescens* ($n = 4$), *A. buddemeieri* ($n = 1$), and *A. elegantissima* ($n = 4$); Jclade: gene sets present in *A. nigrescens* and

A. buddemeieri, and absent in *A. elegantissima*. Gene ratios are presented without confidence intervals, as enrichment calculations were based on pooled genes per group.

Intriguingly, GO terms such as defense response to virus (GO:0051607), regulation of endocytosis (GO:0030100), and regulation of ARF protein signal transduction (GO:0032012) are enriched in both *A. nigrescens*-specific and J clade groups at similar level of enrichment, although the GO term "regulation of ARF protein signal transduction" shows slightly higher enrichment in the *A. nigrescens*-specific gene set. ARF (ADP-ribosylation factor) proteins govern vesicular traffic and organelle structure through the recruitment of coat proteins, modulation of phospholipid metabolism, and alteration of actin structure on membrane surfaces (D'Souza-Schorey and Chavrier 2006). While these enriched GO terms reflect potential immune and cellular regulatory responses, it is important to recognize that such data capture a snapshot of gene expression at a specific point in time, and may reflect biochemical states unique to the sampled individual. This consideration is especially relevant given previous studies in sea anemone venom transcriptomics, which frequently report upregulated defensins, antimicrobial peptides, and other innate immune components as part of venom-related gene expression profiles (Mitchell et al. 2019; Sintsova et al. 2018). The enriched GOs involved in the defense response to virus and regulation of endocytosis could therefore either reflect conserved venom-related expression or species-specific adaptations to the environmental pressure in the Central to Southwest Pacific. Further investigation will be needed to disentangle these possibilities.

DISCUSSION

From the Taiwanese seas, the animals we encountered and collected from both intertidal rocky shore and hydrothermal vents were identified as *A. nigrescens*, based on comparisons to the holotype, other specimens identified as the species from the region, and published description. A key taxonomic feature uniting all live individuals examined is the presence of distinct marginal acrohagi that are noticeably lighter in color – white – than the rest of the column. This characteristic sets them apart from other known *Anthopleura* species reported in nearby waters (*e.g.*, *A. asiastica*, *A. handi*, etc.).

Broadly, taxonomic evidence gathered from the Taiwanese specimens agreed to the holotype, those collected elsewhere (*e.g.*, Singapore, Saudi Arabia), and to data previously published on the species. Some morphological deviations were observed; however, these were largely exhibited in asexual clones. Considering its ability to reproduce asexually and be morphologically variable, we report taxonomical characters that were previously not mentioned in

published detailed redescriptions of the species (*e.g.*, Dunn 1974; England 1987). We found most variability in the cnidom reported, which we attribute to the ongoing confusion surrounding the nomenclature of cnidae.

Regarding transcriptomic analyses, while *A. nigrescens* exhibits enriched genes associated with functions potentially crucial for adaptation to vent environments, enriched GOs restricted to the J clade suggest that *A. nigrescens* and *A. buddemeieri* may utilize similar molecular mechanisms, possibly related to their biogeography. The phylogenetic analysis also indicates that these species are not closely related to the other species (*A. elegantissima* in the EP clade, distributed in the Northeast Pacific Ocean) for which transcriptomic data is available. In fact, the analysis suggests two colonization events, with species from the Southern and Central West Pacific (*A. handi*, *A. nigrescens*, and *A. buddemeieri*) forming a group that is distinct from the species group (*A. elegantissima*, *A. dowii*, and *A. sola*) from the North East Pacific (Daly et al. 2017; Geller and Walton 2001). While additional data is needed to confirm the diversification of *Anthpleura* in distinct geological regions, the transcriptomic data in this study provides the initial glimpse into the genetic diversification of the species in the West Pacific.

Phylogeny of *Anthopleura*

Our phylogenetic reconstruction of *Anthopleura* supports the genus' polyphyly, consistent with previous findings (*e.g.*, Daly et al. 2017; Yap et al. 2023). Notably, the clades within *Anthopleura* appear to cluster geographically: species from the tropical Central Indo-Pacific marine realm are distinct from those in the Tropical Eastern Pacific, Tropical Atlantic, Temperate Southern Africa, and Temperate Northern Pacific (see Spalding et al. 2007 for definitions on marine realms). A particularly unexpected result was the placement of *A. nigrescens* from the Galápagos (Accession number: KY789278, KY789343, KY789373) within the A clade, which is primarily composed of species whose type localities are centered around the Atlantic and African coasts. This contrasts with Daly et al. (2017), where *A. nigrescens* (Galapagos) clustered with Indo-Pacific species such as *Stichodactyla* sp.

Overall, our results reinforce previous studies showing that *Anthopleura* is paraphyletic (Fig. 1), highlighting the need for a comprehensive taxonomic revision of the 49 nominal species currently recognized within the genus. While such a revision is beyond the scope of this study, our findings provide additional evidence supporting the reevaluation of species boundaries and phylogenetic relationships within *Anthopleura*.

Taxonomic characters of *Anthopleura nigrescens*

The external appearance of the specimens we studied from Taiwan and elsewhere (*i.e.*, Saudi Arabia and Singapore) was consistent with the holotype and the details provided in the original description of the species by Verrill (1928). Our observations also align with those of Dunn (1974) and Fautin et al. (2009). Notably, England (1987) did not provide a detailed description of the external appearance of the species, as his focus was primarily on the microanatomy of *A. nigrescens*.

The most distinctive features of this species are the color and appearance of its column and acrohagi. While color is generally not considered a reliable diagnostic character for sea anemones (Stephenson 1928), it appeared consistent among the individuals we examined. Verrill (1928: 26) described the column as "… very dark or smoky brown, or nearly black," which matches the coloration observation in collected specimens from Taiwan, Saudi Arabia, and Singapore. Dunn (1974: 377) was the first to describe the appearance of the acrorhagi, noting them as "… white-tipped, which may have a pinkish cast in specimens with a reddish column,". In later works (*e.g.*, Fautin et al. 2009), they are described more simply as 'white-tipped'. We observed similar features in our specimens, although in some individuals the acrorhagi appeared as a lighter shade than the column, with coloration varying slightly depending on the degree of contraction. Likewise, the purple tinge in the tentacles, as reported by Verrill (1928) in some individuals he examined, was also observed in the specimens we studied (*e.g.*, Fig. 4A).

Verrill (1928), Dunn (1974) and England (1987) reported that the species exhibits a variable number of tentacles. We found this to be accurate; however, none of the individuals we examined had more than 48 tentacles. This variability in tentacle number may reflect its mode of reproduction. As seen in other species that reproduce by longitudinal fission (*e.g.*, *Heteranthus verruculatus* Klunzinger, 1877; see Yap et al. 2021), resulting clones often display asymmetry and variation in external morphology.

Variation associated with asexual reproduction also extends to differences in the internal anatomy of these animals. Both Dunn (1974) and England (1987) noted that the directive mesenteries were not attached to the siphonoglyphs. While this was true for most specimens we examined, we observed an exception in one individual (ZRC.1234). Regarding the retractor muscle, Dunn (1974) alluded to a distinctive free flap, or 'lip', as we refer to it in this study, present on the more developed retractor muscles of this species. Although we observed this feature in our material, it was subtle, and we do not consider it a consistent diagnostic for the species. Moreover, similar structures have been reported in other sea anemone species (*e.g.*, *Macrodactyla fautinae*; see Yap et al. 2023: Fig. 10). Therefore, we suggest that the use of histological characters in sea anemone taxonomy requires careful evaluation.

The occurrence and distribution of cnidae type in our study differ somewhat from those reported by Dunn (1974) and England (1987). As noted earlier, we attribute these discrepancies to differences in cnidae nomenclature used by the authors and the varying standards by which cnidom data are organised and presented. For example, while both Dunn (1974) and England (1987) presumably recorded atriches in the marginal acrorhagi, we identified holotrichs – it is likely that the same cnida type was observed but labelled differently. Another example concerns tentacle spirocysts: we reported two size classes, whereas both Dunn (1974) and England (1987) described only one. Nevertheless, the size ranges we measured are consistent with many previously published values, particularly for basitrichs and spirocysts in the tentacle tip (Table 1). Furthermore, cnidae sizes in specimens from intertidal and hydrothermal vent habitats showed considerable overlap. Overall, our cnidom data are broadly consistent with those reported for the holotype and other voucher specimens examined by Dunn (1974) and England (1987), despite variations in terminology and data presentation.

Transcriptomic aspect

There are significantly enriched GO terms involved in cell proliferation and energy transduction in the *A. nigrescens*-specific orthologous groups. For instance, kinases catalyze the transfer of phosphate from ATP, coordinating various cellular processes such as cell signaling, cell division, growth, and death. The enriched genes associated with the GO term “Dynein intermediate chain binding” may indicate a role in cell division, with the intermediate chain mediating the interaction of cytoplasmic dynein with membranous organelles and kinetochores. Additionally, the enriched GO term “Phosphatidylcholine biosynthetic process” was observed. Phospholipids are essential during cellular growth as they constitute the major components of the cell membrane. Phospholipid metabolism also plays a critical role in lipid regulation and energy metabolism (van der Veen et al. 2017). Phosphatidylcholine, one the most abundant phospholipids in eukaryotic cell membranes, comprises approximately 50% of phospholipid mass (Henneberry et al. 2002). The conversion of phosphocholine to phosphatidylcholine requires ATP (Vance 1989). Since this species lacks photosynthetic endosymbionts, the observed active cell proliferation and energy transduction suggest that it utilizes alternative nutrient and energy sources to support metabolic demands. Indeed, a study on the vent-obligate crab shows it can utilize the vent-associated particulate organic matter (vent POM) for 6-87% of its diet (Chang et al. 2018). Vent POM could similarly serve as an important energy source for *A. nigrescens* inhabiting this environment. Supporting this, Wang et al. (2022) indicated that sea anemones at the Kueishan Island vents feed on both zooplankton and algae in the central vent region, while those in peripheral regions rely primarily on zooplankton. This

dietary shift reflects the environmental heterogeneity on the vent system and may influence local adaptation in *A. nigrescens*.

Ectoderm animals expend a significant amount of energy on thermal regulation in response to ambient temperature environments, as temperature can regulate cellular metabolism or energy budgets (Huey and Kingsolver 2019). Verberk et al. (2016) demonstrated that poor oxygenation drastically reduces in aquatic ectoderms under warm water conditions, suggesting that oxygen limitation impairs survival at thermal extremes and restricts species abundance. Furthermore, a study indicated that species from the hydrothermal vents and shallow water display similar oxygen consumption rates, suggesting that the hydrothermal vent species are more sensitive to temperature variation than those from shallow water (Le Layec and Hourdez 2021). These findings underscore the critical role of temperature and oxygen availability in shaping the physiological responses of ectoderm animals to environmental stressors.

Additionally, the GO "metal ion binding" is highly enriched, potentially shedding light on the biological consequences of the sea anemone's adaptation to the metal-rich environment of the hydrothermal vent. Hydrothermal vent environments are known to have naturally high concentrations of various metals, including Fe, Mn, As, Y, and Ba (Chan et al. 2016; Chen et al. 2018). Studies on vent crabs off Kueishan Island have indicated that metals such as Fe, Cd, Al, and Co accumulated primarily in the gills, while Mn is highest in the exoskeleton, suggesting metal accumulation through the respiration pathway rather than food uptake (Peng et al. 2011). A recent study on sea anemones inhabiting the deep-sea hydrothermal vent revealed genomic data indicating gene family expansions and gene innovations in response to high metal concentration (Zhou et al. 2023). This high-metal environment likely exerts distinct influences on the genetic adaptations of vent animals. The identification of these enriched GO terms sheds light on the cellular mechanisms underlying cell proliferation, membrane biosynthesis, energy metabolism, and metal ion binding in *A. nigrescens*, offering valuable insights into its physiological adaptations to the vent environment and potentially informing future studies on the molecular responses of marine organisms to extreme environments. Although GO analysis does not impose a minimum sample size requirement, the reliability of GO enrichment depends on the robustness of the input gene list, which can be influenced by limited sampling. Therefore, while our analysis identified biologically meaningful categories, these findings should be interpreted with caution. Additional sampling will help validate the generality and strength of the observed expression patterns.

Among the enriched GO terms, those associated with actin dynamics warrant particular attention given their potential link to cellular behavior observed in the field. The enriched GOs related to actin filament binding, organization, and vesicle transport along the actin filament suggest enhanced cellular activity. Actin filaments are crucial for determining cell shape, motility, and

intracellular transport processes. During our field survey at Kueishan Island, we observed asexual reproduction in *A. nigrescens* via longitudinal fission (Fig. 3). Although a previous study on the cnidarian *Hydra oligactis* reported increased rates of asexual reproduction under elevated temperatures (Tökölyi 2024), the connection between actin-related gene enrichment and asexual reproduction remains speculative. Alternatively, the enrichment of actin-associated processes may reflect general cellular stress responses, enhanced tissue repair, or adaptations to environmental factors such as hydrodynamic forces or thermal stress at vent sites. The potential relationship between the frequency of asexual reproduction and environmental conditions in shallow-water hydrothermal vents deserves further targeted investigation.

Given the dynamic nature of shallow-water hydrothermal vents, fluctuations in venting activity, temperature, and chemical exposure may lead to temporal variation in gene expression. Although our sampling was standardized to similar tidal phases and conducted during visually stable venting conditions, we acknowledge that unmeasured short-term fluctuations could influence transcriptional responses. Future studies incorporating time-series sampling or environmental sensors would help disentangle transient versus stable gene expression signatures, thereby improving the resolution of adaptation in variable vent environments.

Along with the *A. buddemeieri* transcriptome from the West Pacific Ocean and genetic information from other *Anthopleura* species, the *A. nigrescens* transcriptome in this study enhances our understanding of the genetic diversity of *Anthopleura* across various oceanic regions, spanning from non-vent coastal areas to vent environments. Previous reports have indicated multiple origins for East and West Pacific *Anthopleura* (Daly et al. 2017; Geller & Walton 2001). Considering the diverse species encompassed within the genus *Anthopleura*, which exhibit a spectrum of symbiotic relationships and clonal aggregations, this genus presents an ideal model for exploring the evolutionary dynamics of symbiosis, clonality, and geological diversification across venting and non-venting environments. However, given the limited availability of taxa with suitable markers, further species identification and expanded taxonomic sampling are needed to fully comprehend the evolutionary relationships of this species within its regional counterparts.

CONCLUSIONS

The challenges in the taxonomy of sea anemones include the high morphological resemblance of some distantly related species, the presence of cryptic species due to convergent evolution or phenotypic plasticity, and poorly defined morphological traits for species delimitation. Increasing studies using an integrative approach that combines morphological and molecular

evidence have strengthened the overall taxonomic framework, leading to more comprehensive and accurate species descriptions and classifications (*e.g.*, Rodríguez et al. 2014; Daly et al. 2017; Yap et al. 2023). For instance, the re-examinations of the type specimens or name-bearing types in several actiniarian superfamilies such as Actiniidea and Actinioidea bear further exploration (Rodríguez et al. 2014; Titus et al. 2019).

Transcriptomic data provides a detailed view of the species' molecular responses to its habitat, as well as the adaptive strategies driving diversification, offering insights into species delimitation. For the species in the J clade, which possess diverse biological and morphological characteristics, the inconsistency in the descriptions of original or type specimens from different locations has led to confusion in species identification. Based on transcriptomic analysis, *A. nigrescens* and *A. buddemeieri*, both members of the J clade, exhibited enriched genes associated with virus defense, endocytosis, and ARF protein signal transduction. While these patterns were initially interpreted in a clade-level context, we recognize that such gene expression likely reflects responses to environmental stimuli, particularly those associated with life in shallow-water hydrothermal vents. The enrichment of virus defense genes may indicate adaptation to increased microbial loads in the vent environment, while genes linked to endocytosis and ARF protein signal transduction may support nutrient acquisition, environmental sensing, or stress response mechanisms. Although not all J clade species occupy vent habitats, the observed gene expression profiles in these two species may represent shared physiological responses to similar ecological pressures rather than defining clade-specific traits. These findings, when contextualized with comparative data (see Figs. 6 and 7), contribute to our understanding of potential molecular mechanisms underlying vent-associated adaptation.

The integration of molecular findings offers an opportunity to prompt the re-examination of morphological data, leading to the identification of new diagnostic traits that may have been overlooked. The redescription of *A. nigrescens* provides a comprehensive understanding of its ecology, morphological traits, phylogeny, and molecular features in relation to the habitat, thereby deepening our knowledge of the biology of *Anthopleura*.

Acknowledgments: The authors are grateful to Prof. Li-Lian Liu, Department of Oceanography, National Sun Yat-sen University, for providing the specimens preserved in formalin and for offering logistic assistance with the specimens sampling in Taiwan. We thank Dr Estefania Rodríguez for her assistance in facilitating the study of the holotype of *Tealiopsis nigrescens* (AMNH 1485) at the American Museum of Natural History, New York. The St John's Island National Marine Laboratory provided the facilities necessary for conducting the morphological aspects of this study. This Laboratory is a National Research Infrastructure under the National Research Foundation

(NRF), Prime Minister's Office, Singapore. We thank Prof. Hon-Tsen Yu from the Department of Life Science, National Taiwan University, for providing the high-performance computer used in the preliminary transcriptomics analysis. Finally, we thank the reviewers for their constructive suggestions and comments.

Authors' contributions: LMF conceived the idea of this study, collected fresh specimens from Taiwan, extracted, sequenced and analyzed genetic data, performed the molecular analyses, and drafted and formatted this manuscript. YWLN examined the morphology of specimens, collected individuals from Saudi Arabia and Singapore, and drafted parts of the manuscript.

Competing interests: The authors declare that they have no conflict of interest.

Availability of data and materials: Specimens documented are kept in natural history museums as stated in the paper, while genetic sequences and supplementary materials are in the process of being deposited in GenBank and Zenodo respectively.

Consent for publication: Not applicable.

Ethics approval consent to participate: Not applicable.

REFERENCES

Alexa A, Rahnenfuhrer J. 2024. topGO: Enrichment Analysis for Gene Ontology. R package version 2.59.0. Available at: https://bioconductor.org/packages/topGO. doi:10.18129/B9.bioc.topGO.

Andres A. 1883. Le Attinie. Atti dell' Accademia de Lincei **14:**211–673

Brandt JF. 1835. Polypos, acalephas discophoras et siphonophoras, nec non echinodermata contiens. Prodromus Descriptionis Animalium AB H. Mertensio in Orbis Terrarum Circumnavigatione Observatorum. Sumptibus Adaemiae, Petropoli.

Bolger AM, Lohse M, Usadel B. 2014. Trimmomatic: a flexible trimmer for Illumina sequence data. Bioinformatics **30:**2114–2120. doi:10.1093/bioinformatics/btu170.

Bruce AJ. 2005. Pontoniine shrimps from Papua New Guinea, with designation of two new genera, *Cainonia* and *Colemonia* (Crustacea: Decapoda: Palaemonidae). Mem Queensl Mus **51:**333–383.

Carlgren O. 1900. Ostafrikanische Actinien. Gesammelt von Herrn Dr. F. Stuhlmann 1888 und 1889. Mitt Naturhist Mus **17:**21–144.

Carlgren O. 1949. A survey of the Ptychodactiaria, Corallimorpharia and Actiniaria. K Svenska Vet Akad Hand **1:**1–121.

Chan BKK, Wang T-W, Chen P-C, Lin C-W, Chan T-Y et al. 2016. Community structure of macrobiota and environmental parameters in shallow water hydrothermal vents off Kueishan Island, Taiwan. PLoS ONE **11:**e0148675. doi:10.1371/journal.pone.0148675.

Chang NN, Lin LH, Tu TH, Jeng MS, Chikaraishi Y et al. 2018. Trophic structure and energy flow in a shallow-water hydrothermal vent: Insights from a stable isotope approach. PLoS ONE **13:**e0204753. doi:10.1371/journal.pone.0204753.

Chen CA, Wallace CC, Yu JK, Wei NV. 2000. Strategies for amplification by polymerase chain reaction of the complete sequence of the gene encoding nuclear large subunit ribosomal RNA in corals. Mar Biotechnol **2:**558–570. doi:10.1007/s101260000040.

Chen XG, Lyu SS, Garbe-Schönberg D, Lebrato M, Li XH et al. 2018. Heavy metals from Kueishantao shallow-sea hydrothermal vents, offshore northeast Taiwan. J Mar Syst **180:**211–219. doi:10.1016/j.jmarsys.2016.11.018.

Cocks WP.1851. Actiniæ (or sea-anemones), procured in Falmouth and its neighbourhood, by W. P. Cocks, Esq., from 1843-1849. Annu Rep R Cornwall Polytech Soc **19:**3–11.

Conesa A, Gotz S, Garcia-Gomez, JM, Terol J, Talon M et al. 2005. Blast2GO: a universal tool for annotation, visualization and analysis in functional genomics research. Bioinformatics **21:**3674–3676. doi:10.1093/bioinformatics/bti610.

D'Souza-Schorey C, Chavrier P. 2006. ARF proteins: roles in membrane traffic and beyond. Nat Rev Mol Cell Biol **7:**347–358. doi:10.1038/nrm1910.

Daly M, Chaudhuri A, Gusmão L, Rodríguez E. 2008. Phylogenetic relationships among sea anemones (Cnidaria: Anthozoa: Actiniaria). Mol Phylogenet Evol **48:**292–301. doi:10.1016/j.ympev.2008.02.022.

Daly M, Crowley LM, Larson P, Rodríguez E, Heestand Saucier E et al. 2017. *Anthopleura* and the phylogeny of Actinioidea (Cnidaria: Anthozoa: Actiniaria). Org Divers Evol **17:**545–564. doi:10.1007/s13127-017-0326-6.

Darriba D, Posada D, Kozlov AM, Stamatakis A, Morel B et al. 2020. ModelTest-NG: a new and scalable tool for the selection of DNA and protein evolutionary models. Mol Biol Evol **37:**291–294. doi:10.1093/molbev/msz189.

Duchassaing de Fonbressin P, Michelotti G. 1860. Mémoire sur les Coralliaires des Antilles. Imprimerie Royale, Turin, 89 pp.

Duchassaing de Fombressin P, Michelotti G. 1864. Supplément au mémoire sur les Coralliaires des Antilles. Imprimerie Royale, Turin, 112 pp.

Dunn DF. 1974. Redescription of *Anthopleura nigrescens* (Coelenterata, Actiniaria) from Hawaii. Pacific Science **28:**377–382.

Dunn DF. 1978. *Anthopleura handi* n. sp. (Coelenterata, Actiniaria), an internally brooding, intertidal sea anemone from Malaysia. Wasmann J Bio **35:**54–64.

Dunn DF. 1981. The clownfish sea anemones: Stichodactylidae (Coelenterata: Actiniaria) and other sea anemones symbiotic with pomacentrid fishes. Trans Am Philos Soc **71:**1–115. doi:10.2307/1006382.

Edgar RC. 2004. MUSCLE: Multiple sequence alignment with high accuracy and high throughput. Nucleic Acids Res **32:**1792–1797. doi:10.1093/nar/gkh340.

Emms DM, Kelly S. 2019. OrthoFinder: phylogenetic orthology inference for comparative genomics. Genome Biol **20:**238. doi:10.1186/s13059-019-1832-y.

England KW. 1987. Certain Actiniaria (Cnidaria, Anthozoa) from the Red Sea and tropical Indo-Pacific Ocean. Bull Brit Mus Nat Hist **53:**205–292.

Escobar-Chico M, Soto LA, Vanegas-Pérez C, Estradas-Romeo A. 2019. Heavy metal bioaccumulation in the anemone *Paraphelliactis pabista* Dunn 1982 (Actiniaria: Hormathiidae) from the hydrothermal system of Guaymas Basin, Gulf of California. Bull Environ Contam Toxicol **102:**486–491. doi:10.1007/s00128-019-02588-z.

Eythorsdottir A, Omarsdottir S, Einarsson H. 2016. Antimicrobial activity of marine bacterial symbionts retrieved from shallow water hydrothermal vents. Mar Biotechnol **18:**293–300. doi:10.1007/s10126-016-9695-7.

Fautin DG. 1984. More Antarctic and Subantartic sea anemones (Coelenterata: Corallimorpharia and Actiniaria). Antarct Res Ser **41:**1–42.

Fautin DG. 2005. Three species of intertidal sea anemones (Anthozoa: Actiniidae) from the tropical Pacific: description of *Anthopleura buddemeieri* n. sp., with remarks on *Anthopleura asiatica* and *Gyractis sesere*. Pac Sci **59:**379–391.

Fautin DG. 2016. Catalog to families, genera, and species of orders Actiniaria and Corallimorpharia (Cnidaria: Anthozoa). Zootaxa **4145:**1–449. doi:10.11646/zootaxa.4145.1.1.

Fautin DG, Barber BR (1999). *Maractis rimicarivora*, a new genus and species of sea anemone (Cnidaria: Anthozoa: Actiniaria: Actinostolidae) from an Atlantic hydrothermal vent. Proc Biol Soc Wash, **112:**624–631.

Fautin DG, Tan SH, Tan R. 2009. Sea anemones (Cnidaria: Actiniaria) of Singapore: abundant and well-known shallow-water species. Raffles Bull Zool Suppl **22:**121–143.

Forsskål P. 1775. Descriptiones Animalium Avium, Amphibiorum, Piscium, Insectorum, Vermium; Quae in Itinere Orientali Observait. Mölleri, Havniæ [Copenhagen], 164 pp.

Fu LM, Niu BF, Zhu ZW, Wu ST, Li WZ. 2012. CD-HIT: Accelerated for clustering the next-generation sequencing data. Bioinformatics **28:**3150–3152. doi:10.1093/bioinformatics/bts565.

Geller JB, Walton ED. 2001. Breaking up and getting back together: evolution of symbiosis and cloning in sea anemones (genus *Anthopleura*) inferred from a molecular phylogeny. Evolution **55:**1781–1794. doi:10.1111/j.0014-3820.2001.tb00837.x.

Goffrendi SK, Motooka C, Fike DA, Gusmão LC, Tilic E et al. 2021. Mixotrophic chemosynthesis in a deep-sea anemone from hydrothermal vents in the Pescadero Basin, Gulf of California. BMC Biol **19:**8. doi:10.1186/s12915-020-00921-1.

Grabherr MG, Haas BJ, Yassour M, Levin JZ, Thompson DA et al. 2011. Full-length transcriptome assembly from RNA-Seq data without a reference genome. Nat Biotechnol **29:**644–652. doi:10.1038/nbt.1883.

Grajales A, Rodríguez E. 2014. Morphological revision of the genus *Aiptasia* and the family Aiptasiidae (Cnidaria, Actinaria, Metridioidea). Zootaxa **3826:**55–100. doi:10.11646/zootaxa.3826.1.2.

Gosse PH. 1854. Descriptions of three new species of British Actiniae. Ann Mag Nat Hist, Ser 2 **14:**280–284.

Guzman C, Shinzato C, Lu TM, Conaco C. 2018. Transcriptome analysis of the reef-building octocoral, *Heliopora coerulea*. Sci Rep **8:**8397. doi:10.1038/s41598-018-26718-5.

Haas BJ, Papanicolaou A, Yassour M, Grabherr M, Blood PD et al. 2013. De novo transcript sequence reconstruction from RNA-seq using the Trinity platform for reference generation and analysis. Nat Protoc **8:**1494–1512. doi:10.1038/nprot.2013.084.

Haddon AC, Shackleton AM. 1893. Description of some new species of Actiniaria from Torres Straits. Sci Proc R Dublin Soc **8:**116–131.

Han J, Kubota S, Uchida H, Stanley Jr. GD, Yao X et al. 2010. Tiny sea anemone from the lower Cambrian of China. PLoS ONE **5:**e13276. doi:10.1871/journal.pone.0013276.

Henneberry AL, Wright MM, McMaster CR. 2002. The major sites of cellular phospholipid synthesis and molecular determinants of Fatty Acid and lipid head group specificity. Mol Biol Cell **13:**3148–3161. doi:10.1091/mbc.01-11-0540.

Holm NG, Andersson E. 2005. Hydrothermal simulation experiments as a tool for studies of the origin of life on Earth and other terrestrial planets: a review. Astrobiology **5:**444–160. doi:10.1089/ast.2005.5.444.

Huey RB, Kingsolver JG. 2019. Climate warming, resource availability, and the metabolic meltdown of Ectotherms. Am Nat **194:**E140–E150. doi:10.1086/705679.

Humanson GL. 1967. Animal tissue techniques. Second edition. WH Freeman & Company, San Francisco, California, USA.

Katoh K, Rozewicki J, Yamada KD. 2019. MAFFT online service: Multiple sequence alignment, interactive sequence choice and visualization. Brief Bioinform **20:**1160–1166. doi:10.1093/bib/bbx108.

Klunzinger CB. 1877. Die Korallthiere des rothen Meeres, 1: Die Alcyonarien und Malacodermen. Verlag der Gutmann'schen Buchhandlung, Berlin, 98 pp.

Le Layec V, Hourdez S. 2021. Oxygen consumption rates in deep-sea hydrothermal vent scale worms: Effect of life-style, oxygen concentration, and temperature sensitivity. Deep-Sea Res I:Oceanogr Res Pap **172:**103531. doi:10.1016/j.dsr.2021.103531.

Lesson RP. 1830. Description des animaux de la famille des Actiniées. Voyage Autour du Monde, Exécuté par Ordre du Roi, sur la Corvette de La Majesté, La Coquille, pendant les années 1822, 1823, 1824, et 1825, sous le ministère et conformément aux instructions de S. E. M. de Marquis de Clermont-Tonnerre, ministre de la marine. Arthus Bertrand, Paris, pp. 67–83.

Li WZ, Godzik A. 2006. CD-hit: a fast program for clustering and comparing large sets of protein or nucleotide sequences. Bioinformatics **22:**1658–1659. doi:10.1093/bioinformatics/btl158.

Liu C, Bian C, Gao Q, Gao Z, Huang Y et al. 2024. Whole genome sequencing of a novel sea anemone (Actinostola sp.) from a deep-sea hydrothermal vent. Sci Data **11:**102. doi:10.1038/s41597-024-02944-7.

López-González PJ, Rodríguez E, Segonzac M. 2005. A new species of sea anemone (Cnidaria: Anthozoa: Actiniaria) from Manus Basin hydrothermal vents, South-western Pacific. Mar Biol Res **1:**326–337. doi:10.1080/17451000500380306.

López-González PJ, Rodríguez E, Gili JM, Segonzac M. 2003. New records on sea anemones (Anthozoa: Actiniaria) from hydrothermal vents and cold seeps. Zool Verh **345:**215–243.

Macrander JC, Brugler MR, Daly M. 2015. A RNA-seq approach to identify putative toxins from acrorhagi in aggressive and non-aggressive *Anthopleura elegantissima* polyps. BMC Genomics **16:**221. doi:10.1186/s12864-015-1417-4.

Macrander JC, Dimond JL, Bingham BL, Reitzel AM. 2018. Transcriptome sequencing and characterization of *Symbiodinium muscatinei* and *Elliptochloris marina*, symbionts found within the aggregating sea anemone *Anthopleura elegantissima*. Mar Genomics **37:**82–91. doi:10.1016/j.margen.2017.08.010.

Mariscal RN. 1974. Nematocysts. *In*: Muscatine L, Lenhoff HM (eds) Coelenterate Biology: Reviews and New Perspectives. Academic Press Inc, New York, pp. 129–178.

Mitchell ML, Shafee T, Papenfuss AT, Norton RS. 2019. Evolution of cnidarian trans-defensins: Sequence, structure and exploration of chemical space. Proteins: Structure, Function, and Bioinformatics **87:**551–560. doi:10.1002/prot.25679.

Peng SH, Hung JJ, Hwang J-S. 2011. Bioaccumulation of trace metals in the submarine hydrothermal vent crab *Xenograpsus testudinatus* off Kueishan Island, Taiwan. Mar Pollut Bull **63:**396–401. doi:10.1016/j.marpolbul.2011.05.013.

Riemann-Zürneck K. 1986. On some abyssal sea anemones of the North Atlantic (Actiniaria: Hormathiidae). Mitt zool Mus Hamburg **83:**7–29.

Rodríguez E, Barbeitos MS, Brugler MR, Crowley LM, Grajales A et al. 2014. Hidden among sea anemones: the first comprehensive phylogenetic reconstruction of the order

Actiniaria (Cnidaria, Anthozoa, Hexacorallia) reveals a novel group of hexacorals. PLoS ONE **9:**1–7. doi:10.1371/journal.pone.0096998.

Rodríguez E, Castorani CN, Daly M. 2008. Morphological phylogeny of the family Actinostolidae (Anthozoa: Actiniaria) with description of a new genus and species of hydrothermal vent sea anemone redefining the family Actionscyphiidae. Invertebr Syst **22:**439–452. doi:10.1071/IS07053.

Rodríguez E, Barbeitos M, Daly M, Gusmão LC, Häussermann V. 2012. Toward a natural classification: phylogeny of acontiate sea anemones (Cnidaria, Anthozoa, Actiniaria). Cladistics **28:**375–392. doi:10.111/j.1096-0031.2012.00391.x.

Ronquist F, Huelsenbeck JP. 2003. MRBAYES 3: Bayesian phylogenetic inference under mixed models. Bioinformatics **19:**1572–1574. doi:10.1093/bioinformatics/btg180.

Sintsova O, Gladkikh I, Chausova V, Monastyrnaya M, Anastyuk S et al. 2018. Peptide fingerprinting of the sea anemone *Heteractis magnifica* mucus revealed neurotoxins, Kunitz-type proteinase inhibitors and a new β-defensin α-amylase inhibitor. Journal of Proteomics **173:**12–21. doi:10.1016/j.jprot.2017.11.019.

Spalding MD, Fox HE, Allen GR, Davidson N, Ferdaña ZA et al. 2007. Marine ecoregions of the world: a bioregionalization of coastal and shelf areas. Bioscience **7:**573–583. doi:10.1641/B570707.

Stamatakis, A. 2014. RAxML version 8: a tool for phylogenetic analysis and post-analysis of large phylogenies. Bioinformatics **30:**1312–1313. doi:10.1093/bioinformatics/btu033.

Stephenson TA. 1928. The British sea anemones Volume I. The Ray Society, London, UK.

Stimpson W. 1856. On some remarkable marine invertebrata inhabiting the shores of South Carolina. Proc Boston Soc Nat Hist **5:**110–118.

Sunagawa S, Wilson EC, Thaler M, Smith ML, Caruso C et al. 2009. Generation and analysis of transcriptomic resources for a model system on the rise: the sea anemone *Aiptasia pallida* and its dinoflagellate endosymbiont. BMC Genom **10:**258. doi:10.1186/1471-2164-10-258.

Titus BM, Benedict C, Laroche R, Gusmão LC, Deusen VV et al. 2019. Phylogenetic relationships among the clownfish-hosting sea anemones. Mol Phylogenet Evol **139:**106526. doi:10.1016/j.ympev.2019.106526.

Tarasov VG, Gebruk AV, Mironov AN, Moskalev LI. 2005. Deep-sea and upper sublittoral hydrothermal vent communities. Two different phenomena? Chem Geol **224:**5–39. doi:10.1016/j.chemgeo.2005.07.021.

Tökölyi, J. 2024. Temperature-dependent scaling of fitness traits with body size in hydra. Funct Ecol **38:**245–258. doi:10.1111/1365-2435.14457.

Uchida T. 1938. Actiniaria of Mutsu Bay. Report of the Biological Survey of Mutsu Bay **13:**281–317.

van der Burg CA, Prentis PJ, Surm JM, Pavasovic A. 2016. Insights into the innate immunome of actiniarians using a comparative genomic approach. BMC Genomics **17:**850. doi:10.1186/s12864-016-3204-2.

van der Veen JN, Kenney JP, Wan S, Vance JE, Vance DE et al. 2017. The critical role of phosphatidylcholine and phosphatidylethanolamine metabolism in health and disease. Biochimica et Biophysica Acta (BBA)-Biomembranes **1859:**1558–1572. doi:10.1016/j.bbamem.2017.04.006.

Vance DE. 1989. Phosphatidylcholine metabolism. CRC press.

Verberk WC, Durance I, Vaughan IP, Ormerod SJ. 2016. Field and laboratory studies reveal interacting effects of stream oxygenation and warming on aquatic ectotherms. Glob Change Biol **22:**1769–1778. doi:10.1111/gcb.13240.

Verrill AE. 1883. Report on the Anthozoa, and on some additional species dredged by the "Blake" in 1877–1879, and by the U.S. Fish Commission steamer "Fish Hawk" in 1880-82. Bull Mus Comp Zool Harvard **11:**1–72.

Verrill AE. 1899. Descriptions of imperfectly known and new Actinians, with critical notes on other species, IV. Am J Sci Arts **7:**205–218.

Verrill. AE. 1928. Hawaiian shallow water Anthozoa. Bernice P. Bishop Museum Bulletin **49:**3–30.

Wächtershäuser G. 1988. Before enzymes and templates: theory of surface metabolism. Microbiol Rev **52:**452–484.

Wang TW, Lau DCP, Chang TY, Chan BKK. 2022. Autochthony and isotopic niches of benthic fauna at shallow-water hydrothermal vents. Sci Rep **12:**6248. doi:10.1038/s41598-022-09839-w.

Yanagi K, Daly M. 2004. The hermaphroditic sea anemone *Anthopleura atodai* n. sp. (Anthozoa: Actiniaria: Actiniidae) from Japan, with a redescription of *A. hermaphroditica*. Proc Biol Soc Was **117:**408–422.

Yap NWL, Mitchell ML, Quek ZBR, Tan R, Tan KS et al. 2023. Taxonomy and molecular phylogeny of the sea anemone *Macrodactyla* (Haddon, 1898) (Cnidaria, Actiniaria), with a description of a new species from Singapore. Zool Stud **62:**e29. doi:10.6620/ZS.2023.62-29.

Yap NWL, Quek ZBR, Tan R, Nugroho DA, Lee JN et al. 2021. Carlgren's hesitation allayed: redescription and systematics of *Heteranthus verruculatus* Klunzinger, 1877 (Cnidaria, Actiniaria), with a redefinition of Heteranthidae Carlgren, 1900. Contrib Zool **90:**155–182. doi:10.1163/18759866-BJA10015.

Zhou Y, Liu H, Feng C, Lu Z, Liu J, Huang Y et al. 2023. Genetic adaptations of sea anemone to hydrothermal environment. Sci Adv **9:**eadh0474. doi:10.1126/sciadv.adh0474.

Supplementary materials

Fig. 1. Locations of where specimens of *Anthopleura nigrescens* (Verrill, 1928) were obtained which we had examined in this study. A, Saudi Arabia, 1 = Thuwal (22°20'37.8"N 39°05'18.4"E). B, Singapore, 2 = Pulau Tekkukor (1°13'46.6"N 103°50'22.2"E), 3 = Changi Beach (1°23'32.2"N 103°59'25.7"E), 4 = Changi Point Ferry Terminal (1°23'29.5"N 103°59'14.9"E), 5 = Punggol Beach (1°25'18.9"N 103°54'39.7"E). C, Keuisan Island, Taiwan, 6=intertidal (24°50'36.6"N 121°56'27.0"E), 7 = Hydrothermal vent (24°50'48.8"N 121°56'31.2"E).